Regulation of mitotic recombination between DNA repeats in centromeres

Faria Zafar, Akiko K. Okita, Atsushi T. Onaka, Jie Su, Yasuhiro Katahira, Jun-ichi Nakayama, Tatsuro S. Takahashi, Hisao Masukata and Takuro Nakagawa

Supplementary Data

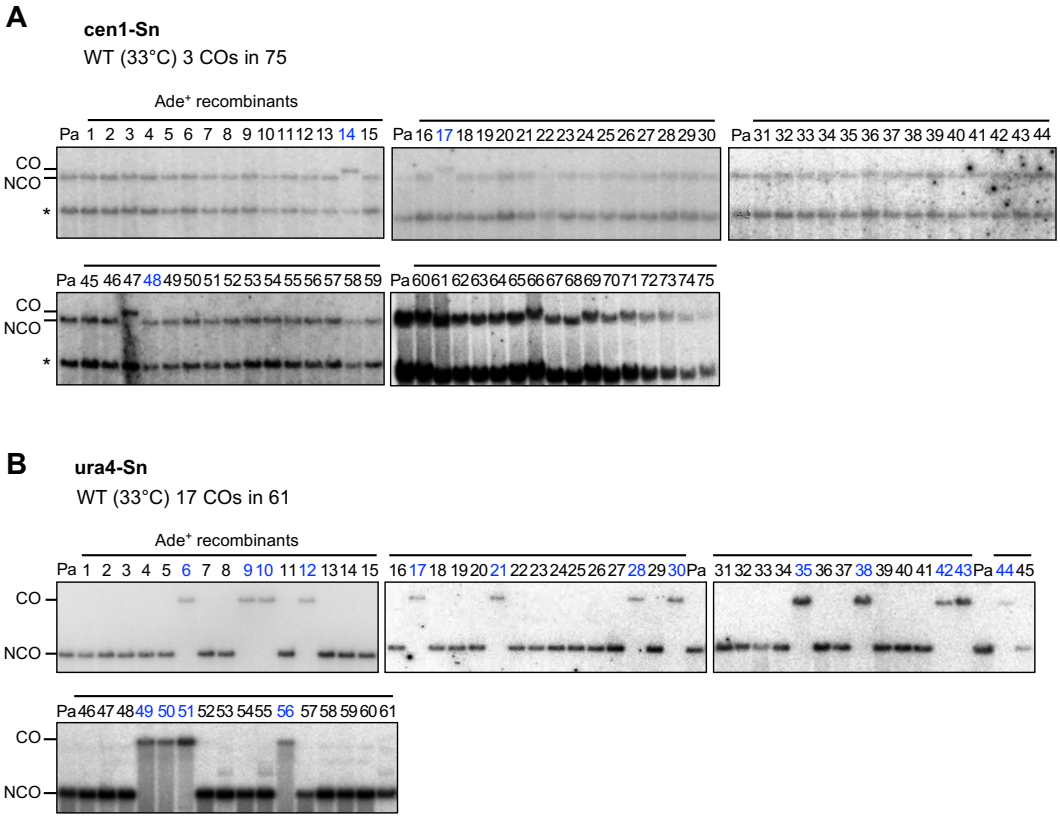

Supplementary Figure S1. Physical detection of crossover and non-crossover recombinants in the cen1-Sn and ura4-Sn constructs in wild type strains. (A) Crossover and non-crossover recombinants produced in the cen1-Sn construct in wild type (TNF3347). Southern hybridization of restriction fragments was carried out as described in Figure 2. (B) Crossover and non-crossover recombinants produced in the ura4-Sn construct in wild type (TNF3631). Crossovers are shown in blue. Pa, parental; *, a band from cnt3. CO, crossover: NCO, non-crossovers.

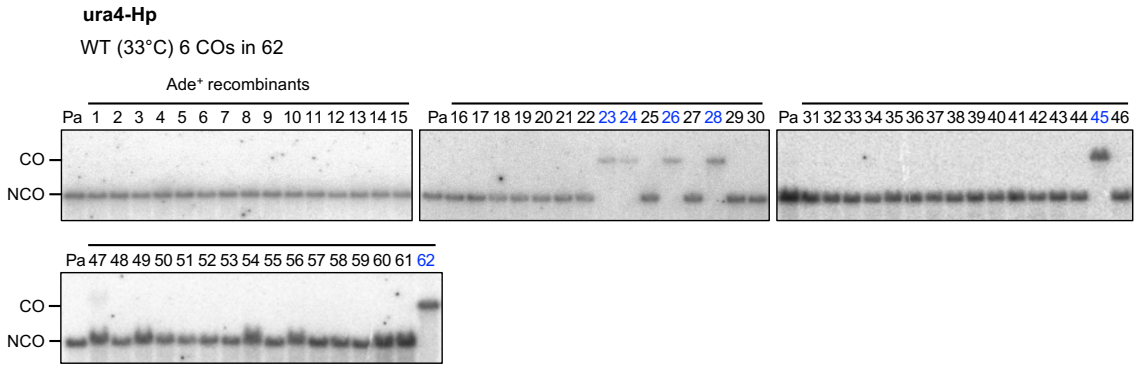

Supplementary Figure S2. Physical detection of crossovers and non-crossovers in the ura4-Sn construct in the wild type strain (TNF3650).

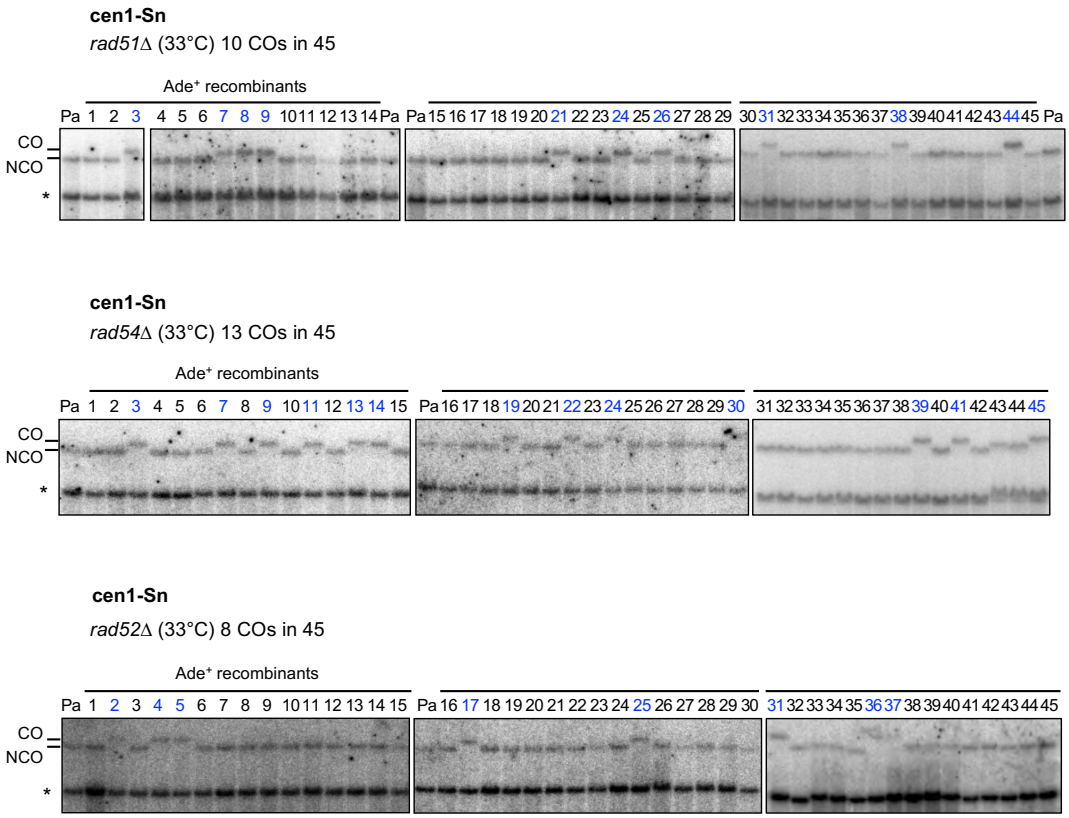

Supplementary Figure S3. Physical detection of crossovers and non-crossovers in the cen1-Sn construct in *rad51*Δ, *rad54*Δ, and *rad52*Δ strains (TNF3446, 3452, and 3459, respectively).

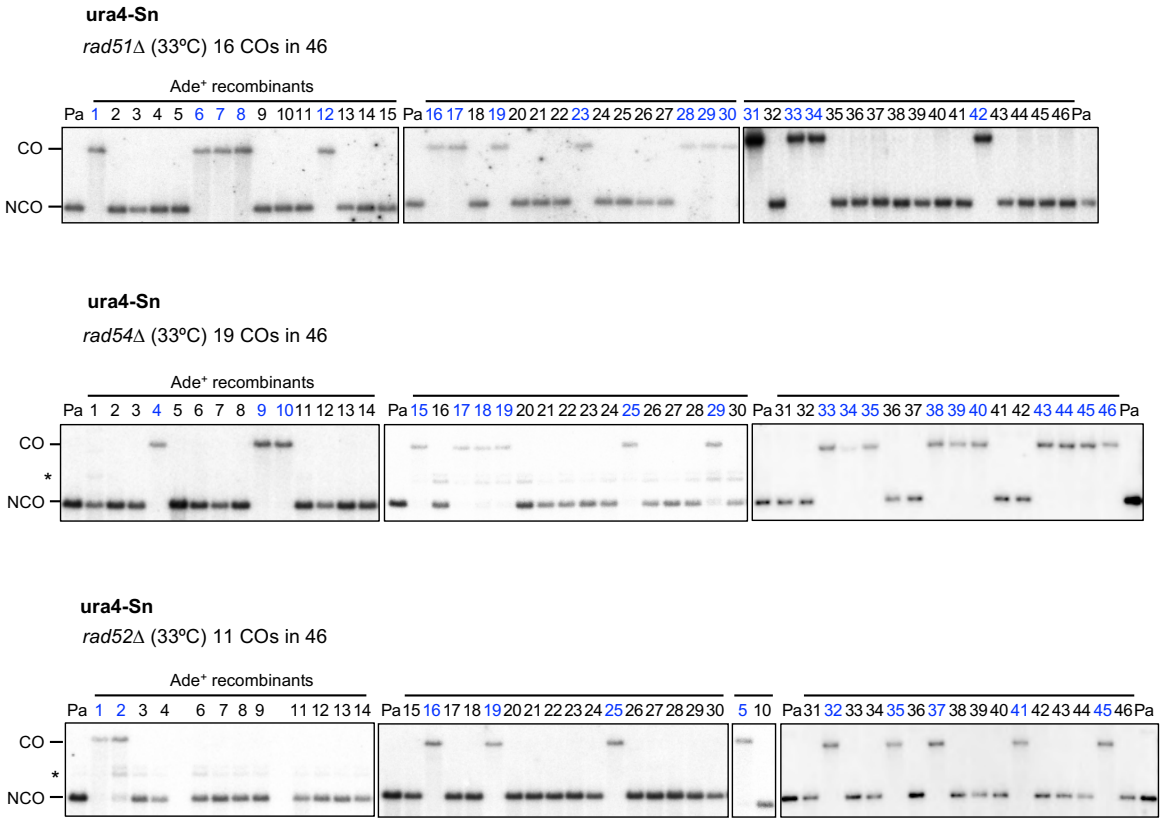

Supplementary Figure S4. Physical detection of crossovers and non-crossovers in the ura4-Sn construct in *rad51*Δ, *rad54*Δ, and *rad52*Δ strains (TNF3635, 3645, and 3643, respectively). *, non-specific band.

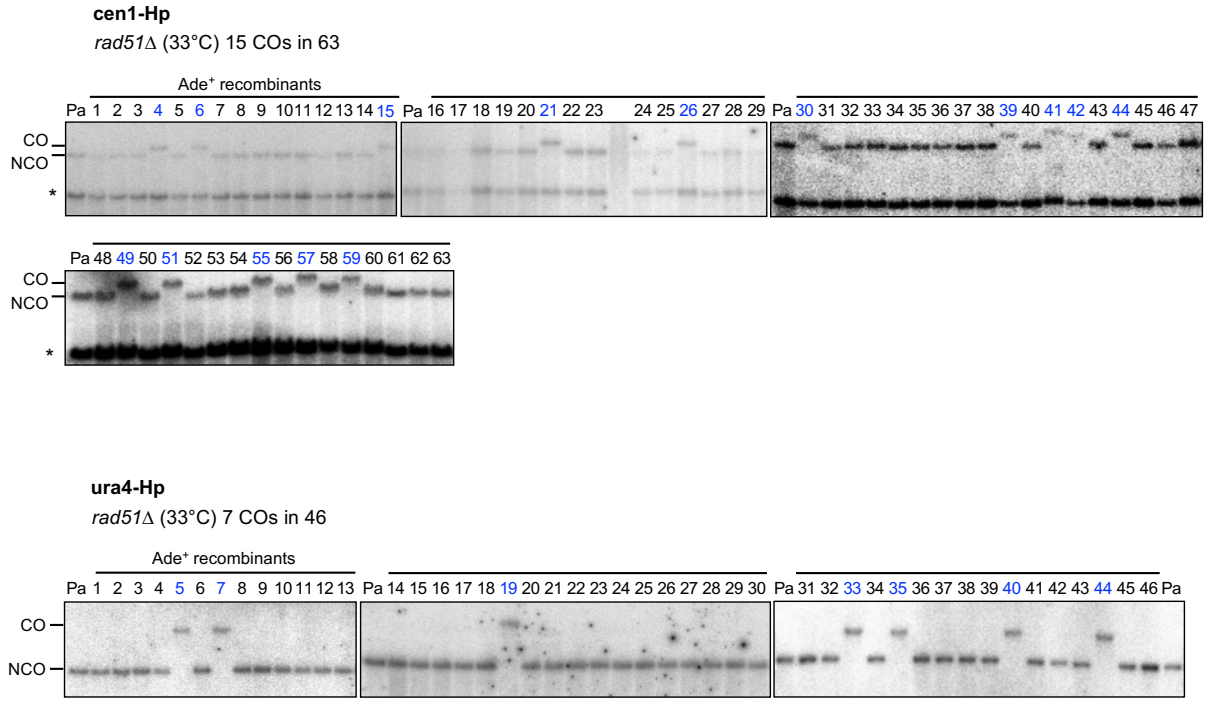

Supplementary Figure S5. Physical detection of crossovers and non-crossovers in the cen1-Hp and ura4-Hp constructs in the *rad51*Δ strains (TNF3257 and 3664, respectively).

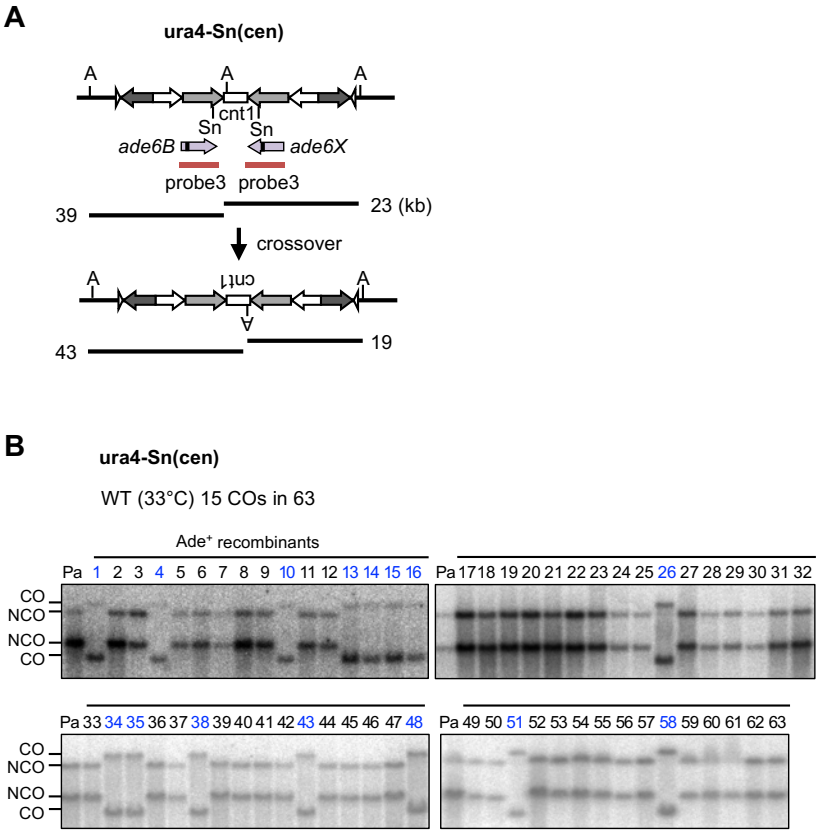

Supplementary Figure S6. Physical detection of crossovers and non-crossovers in the ura4-Sn(cen) construct in the wild type strain (TNF4684). (A) Illustrated is the ura4-Sn(cen) construct. Positions of centromere repeats, AfeI restriction sites, probe3, and the length of AfeI restriction fragments are indicated. *ade6B/X* were omitted in the bottom part of the illustration for simplicity. (B) Southern hybridization of AfeI restriction fragments using probe3.

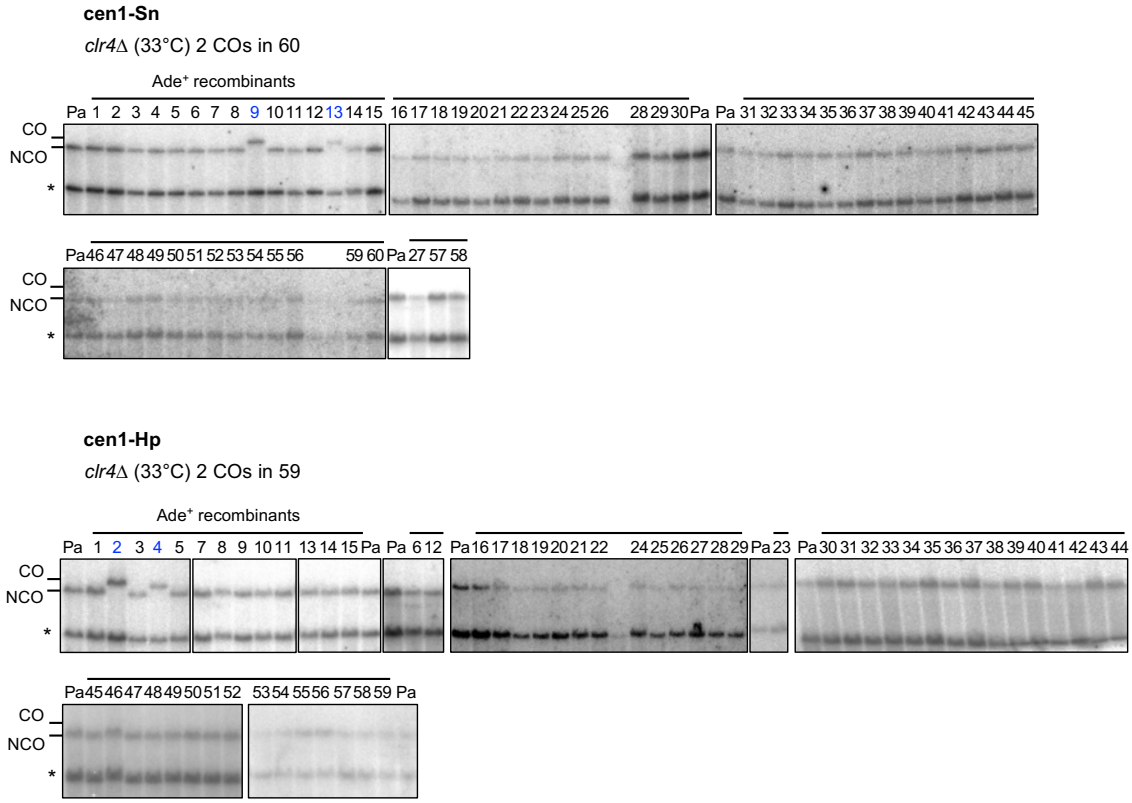

Supplementary Figure S7. Physical detection of crossovers and non-crossovers in the cen1-Sn and cen1-Hp constructs in the *clr4* mutants (TNF3734 and 3550, respectively).

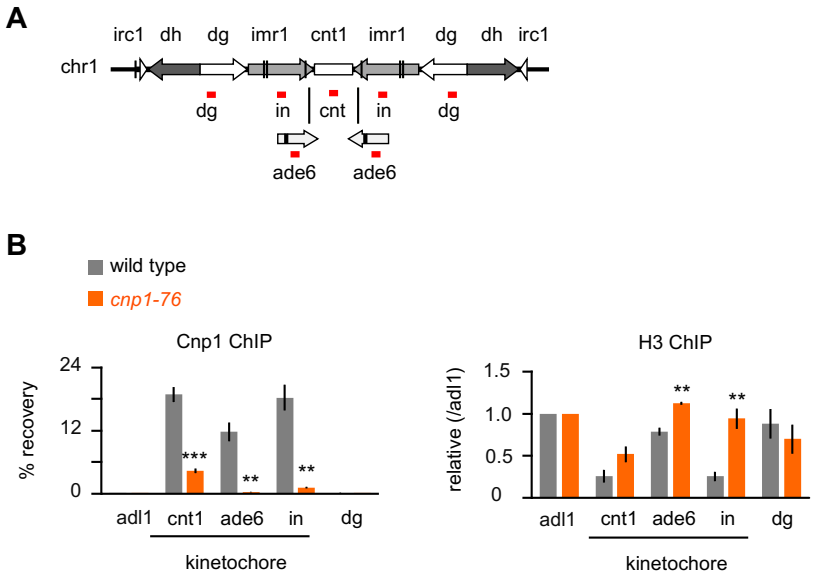

Supplementary Figure S8. The effect of the *cnp1-76* mutation on the localization of Cnp1 and histone H3 in centromeres. (A) Illustrated is the cen1-Sn construct. Positions of centromere repeats, *ade6B/X*, and the regions amplified by real-time PCR are shown. The *adl1* gene is present on the arm of chr2. (B) ChIP experiments were carried out using wild type and *cnp1-76* mutant strains (TNF3347 and 3736, respectively) grown at a semipermissive temperature of 30°C. Mean ± SEM from three independent experiments are shown. ***P* <0.01; ****P* <0.001. *P*-values were determined by the two-tailed student T-test.

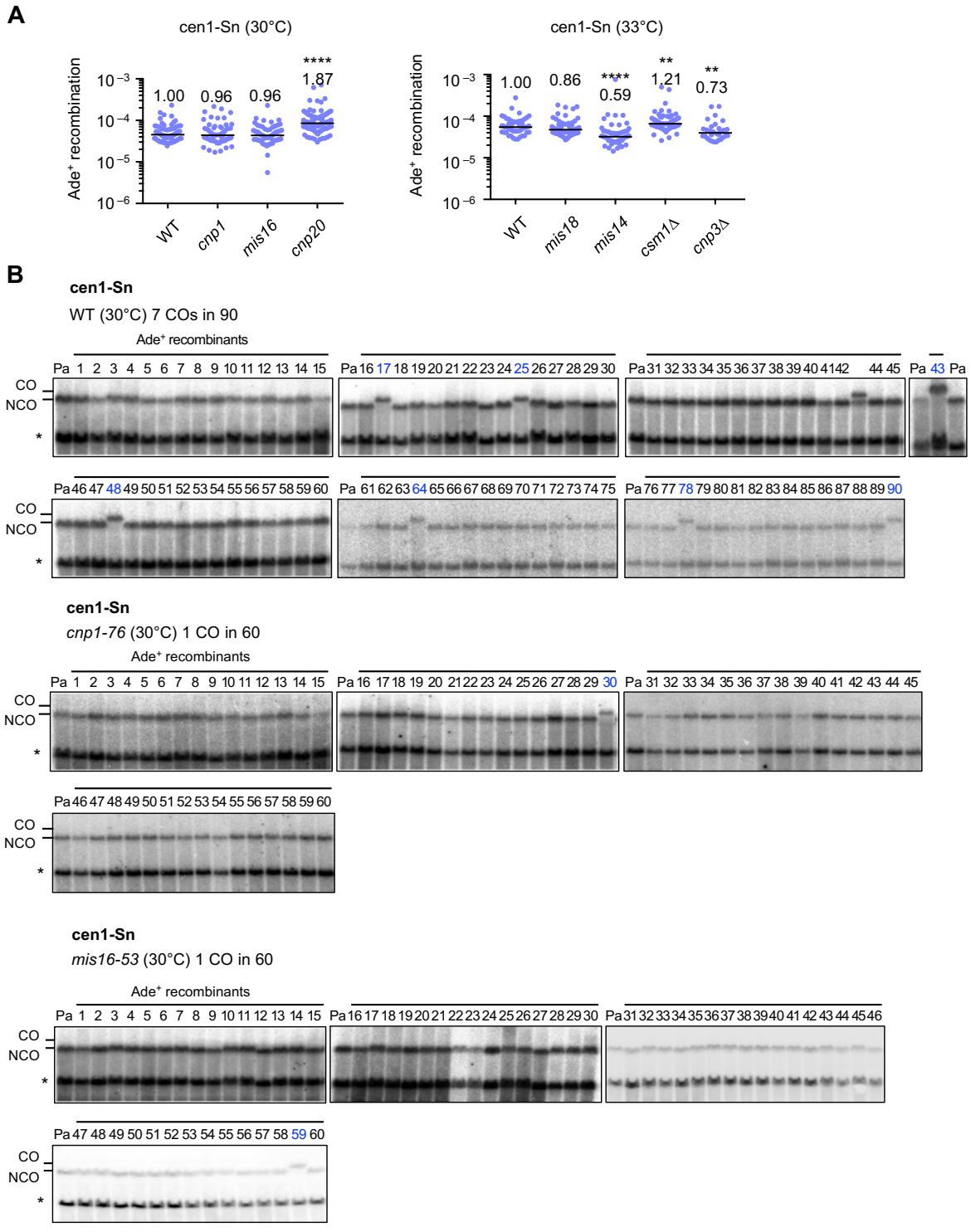

Supplementary Figure S9 (continued)

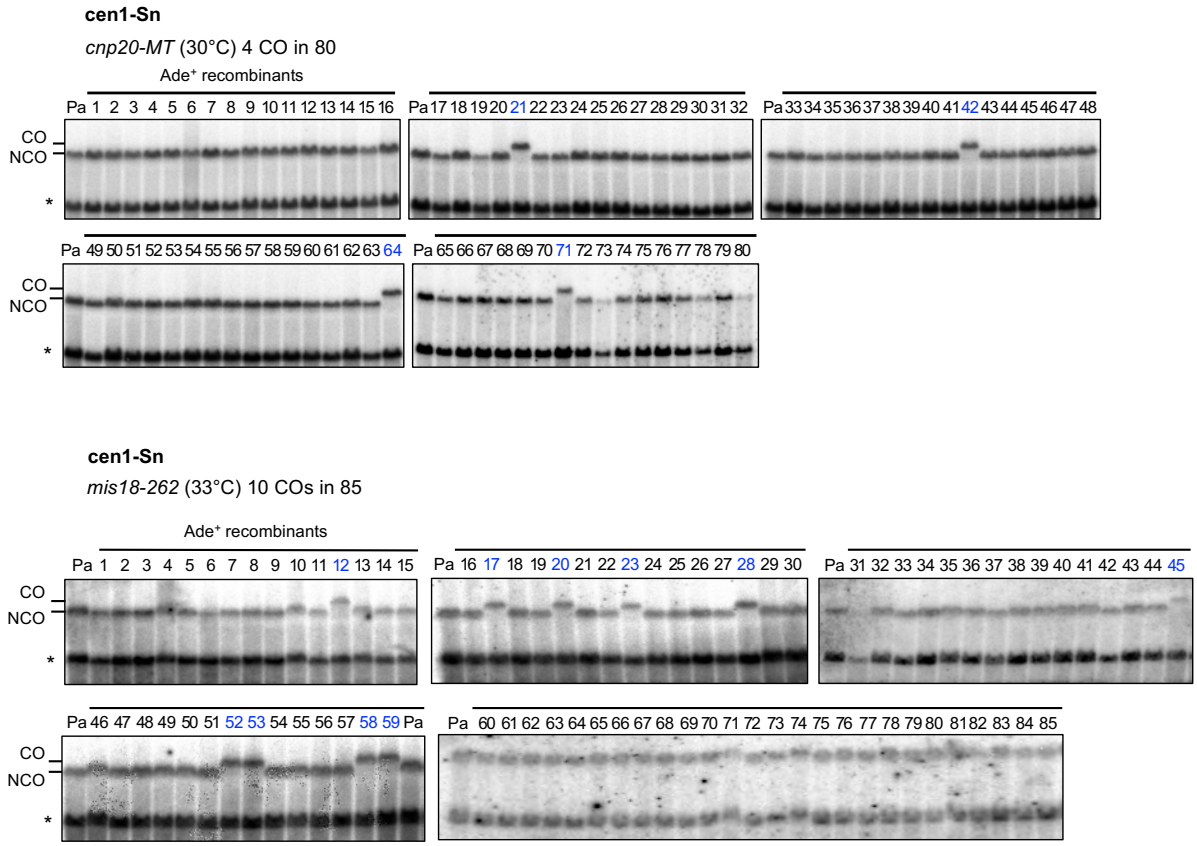

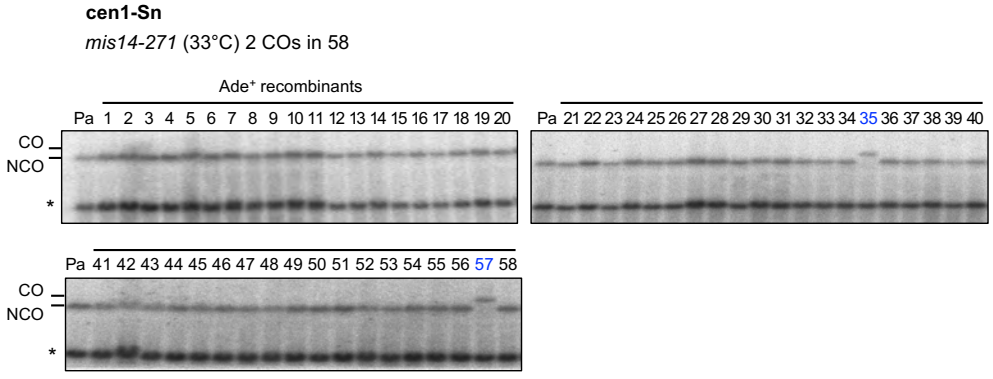

Supplementary Figure S9 (continued)

cen1-Sn
*csm1*Δ (33°C) 5 CO in 59

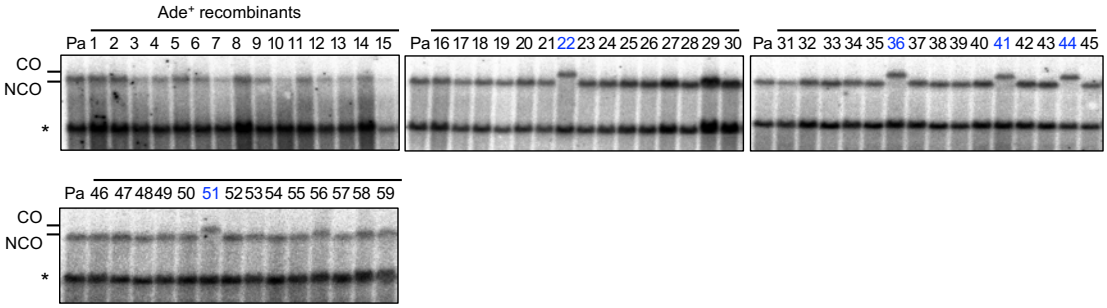

cen1-Sn
*cnp3*Δ (33°C) 1 CO in 30

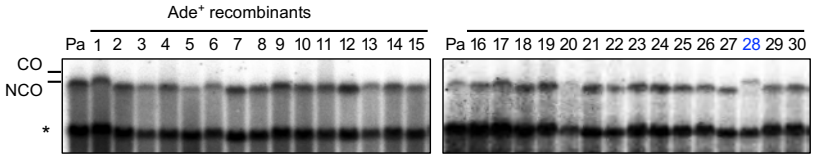

cen1-Sn
WT (28°C) 4 COs in 59

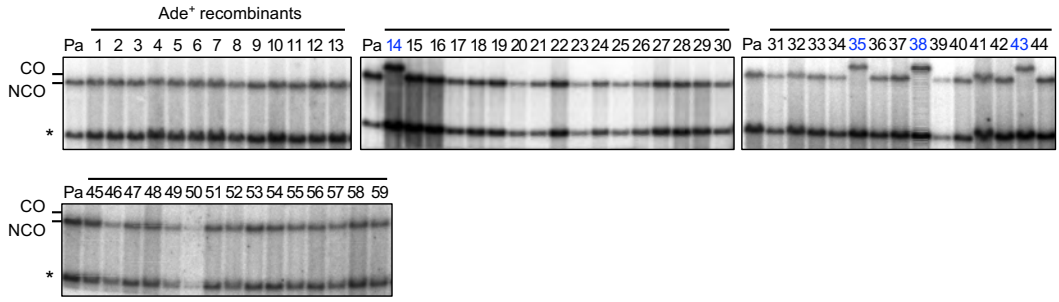

cen1-Sn
*mhf1*Δ (28°C) 16 COs in 61

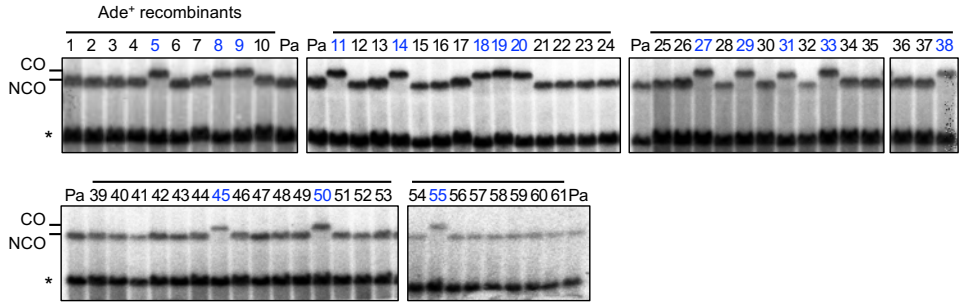

Supplementary Figure S9 (continued)

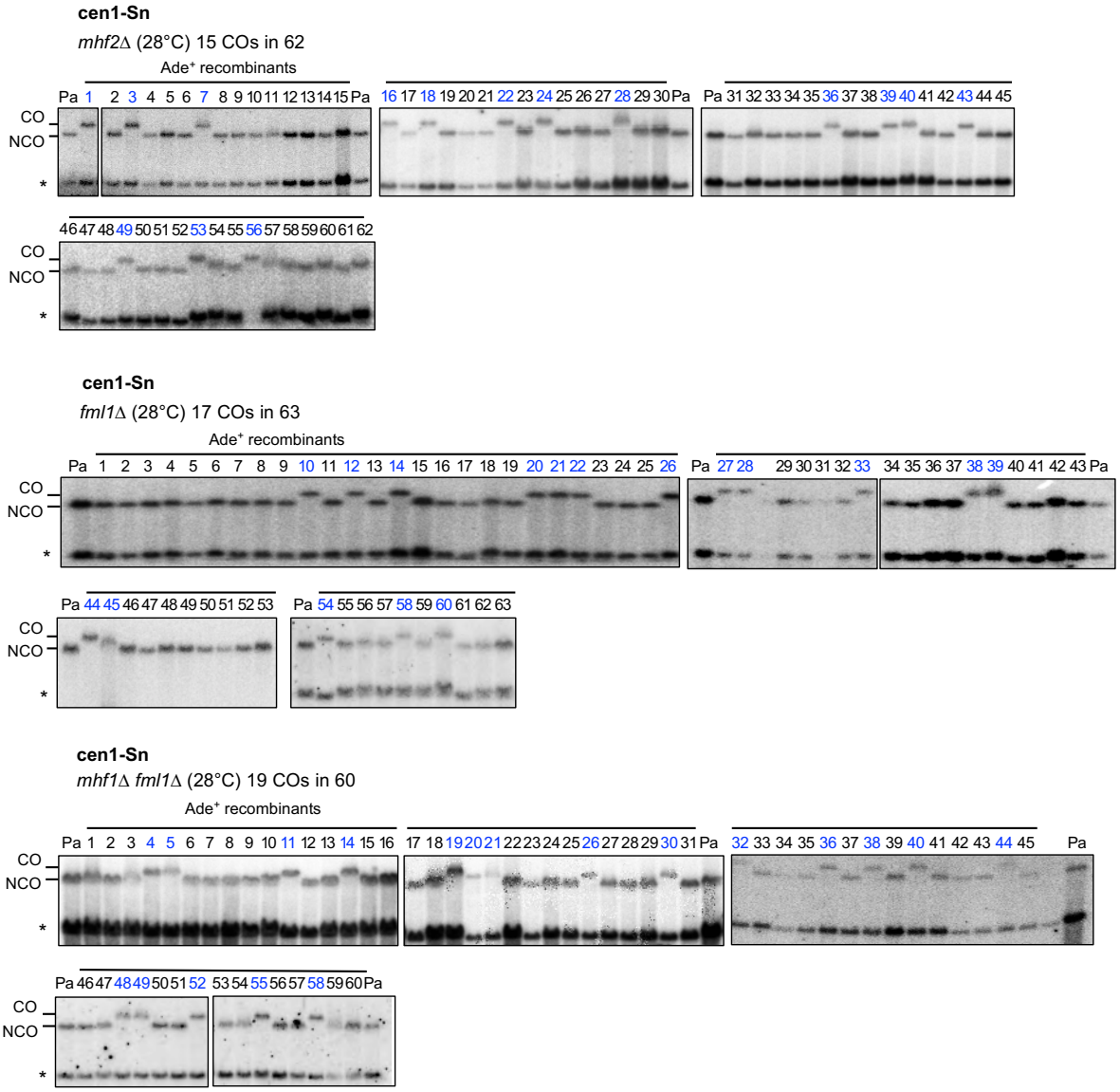

Supplementary Figure S9. The effect of mutations of the centromere protein on crossovers and non-crossovers in the cen1-Sn construct. (A) Recombination rates in wild type, *cnp1-76, mis16-53,* and *cnp20-M447T* strains (TNF3347, 3736, 4656, and 5534, respectively) at 30°C as well as those in wild type, *mis18-262, mis14-271*, *csm1*Δ*,* and *cnp3*Δ (TNF3347, 4657, 5376, 4139, and 4115, respectively) at 33°C. Lines indicate medians. Rates relative to the wild-type value are indicated at the top of each column. *P*-values were determined by the two-tailed Mann-Whitney test. ****P <0.0001. (B) Physical detection of crossovers and non-crossovers in the cen1-Sn construct in wild type, *cnp1-76, mis16-53,* and *cnp20-M447T* strains at 30°C; *mis18-262, mis14-271*, *csm1*Δ*,* and *cnp3*Δ strains at 33°C; wild type*, mhf1*Δ, *mhf2*Δ, *fml1*Δ*,* and *mhf1*Δ *fml1*Δ (T1NF3347, 4779, 5082, 5353, and 5128, respectively) at 28°C.

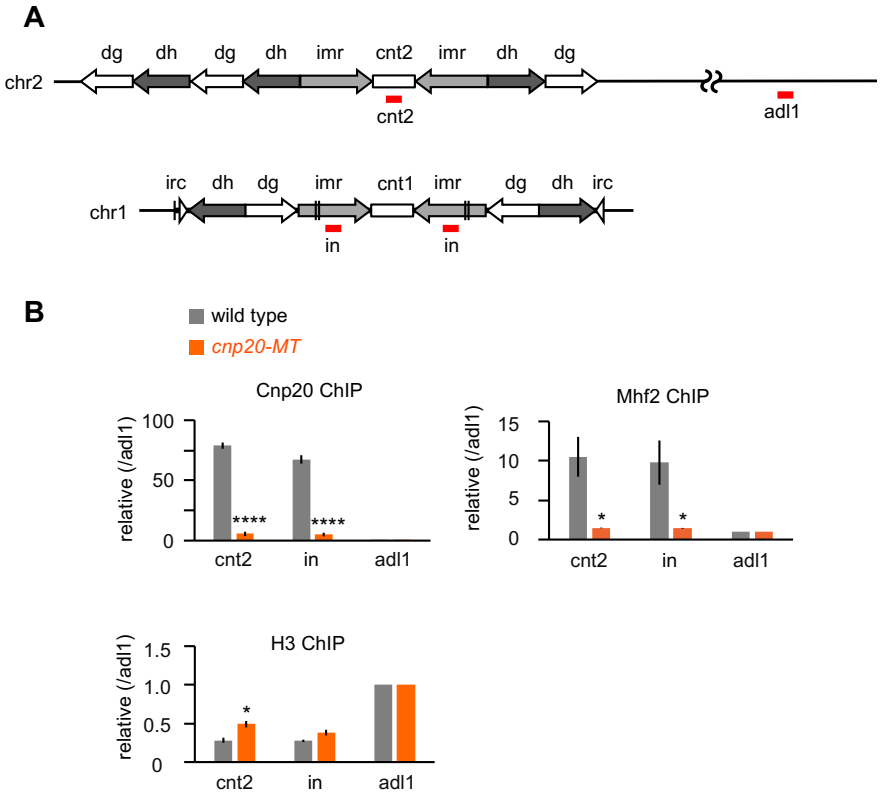

Supplementary Figure S10. The effect of *cnp20-M447T* mutation on the localization of Cnp20, Mhf2, and histone H3 in centromeres. The *cnp20-M447T* mutation changes methionine at 447 of Cnp20/CENP-T to threonine. The *cnp20-M447T* temperature-sensitive mutant was created by the PCR-based mutagenesis of the histone-fold domain of Cnp20. (A) Illustrated are cen1 and cen3. Positions of centromere repeats and the regions that were amplified by real-time PCR are indicated. (B) ChIP experiments were carried out using wild type and *cnp20-MT* mutant strains (TNF35 and 5485, respectively) grown at a semipermissive temperature of 30°C. Mean ± SEM from three independent experiments are shown. *P*-values were determined by the two-tailed student T-test.

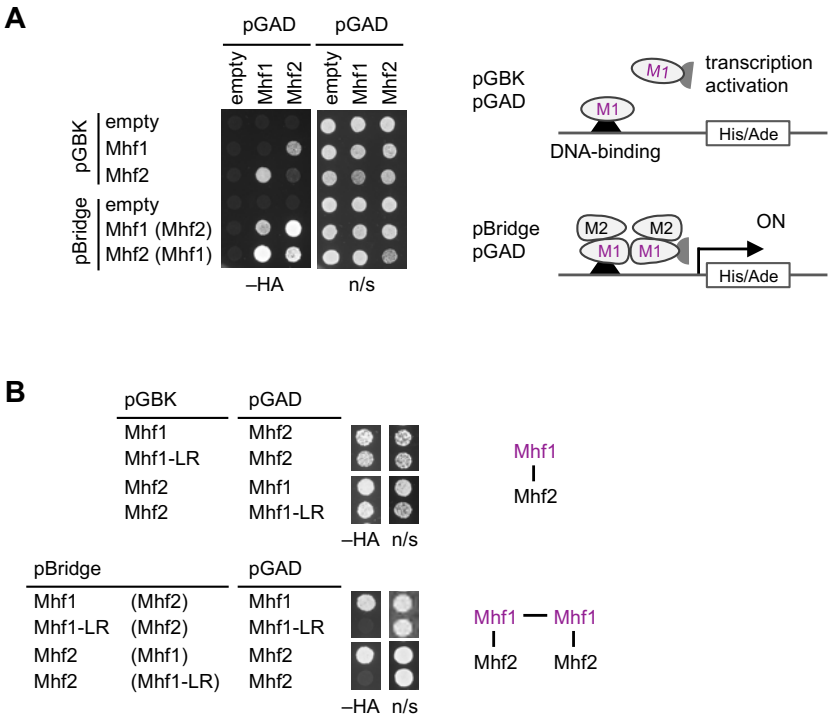

Supplementary Figure S11. Yeast two-hybrid (Y2H) assays to examine Mhf1-Mhf2 dimer and $(Mhf1\text{-}Mhf2)_2$ tetramer formation. Interaction between a pair of fusion proteins that contain a DNA-binding domain or a transcription activation domain allows expression of *HIS3* and *ADE2* reporter genes. Budding yeast cells expressing a pair of fusion proteins were spotted on selective (–HA) and non-selective (n/s) plates. (A) Y2H interaction was observed between Mhf1-Mhf2 but not between the same two subunits (upper half). Consistent with $(Mhf1\text{-}Mhf2)_2$ tetramer formation, however, Mhf1-Mhf1 interaction was detected when Mhf2 was additionally expressed from the pBridge plasmid (lower half). Similarly, Mhf2-Mhf2 interaction was detected when Mhf1 was additionally expressed. Depicted is the interaction between Mhf1 and Mhf1 that is only detected in the presence of Mhf2. Additional non-fusion proteins expressed from pBridge are shown in parentheses. (B) Effects of *mhf1-L78R* mutation on the Y2H interaction among Mhf1 and Mhf2. *mhf1-LR* did not affect Mhf1-Mhf2 interaction (the upper half) but abolished Mhf1-Mhf1 and Mhf2-Mhf2 interaction in the presence of Mhf2 and Mhf1, respectively (lower half). These data suggest that *mhf1-L78R* specifically impairs $(Mhf1\text{-}Mhf2)_2$ tetramer but not Mhf1-Mhf2 dimer formation.

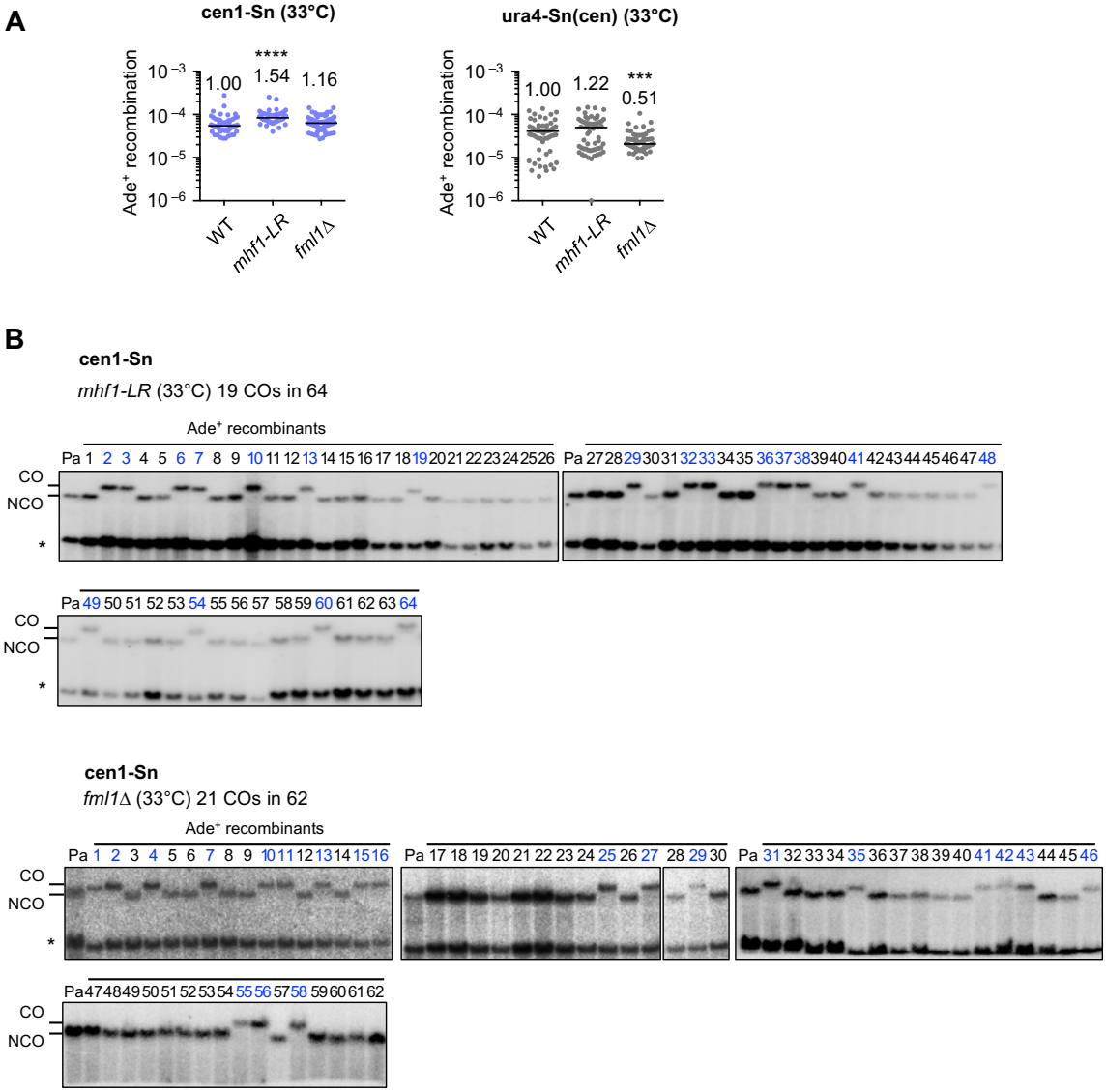

Supplementary Figure S12 (contiued)

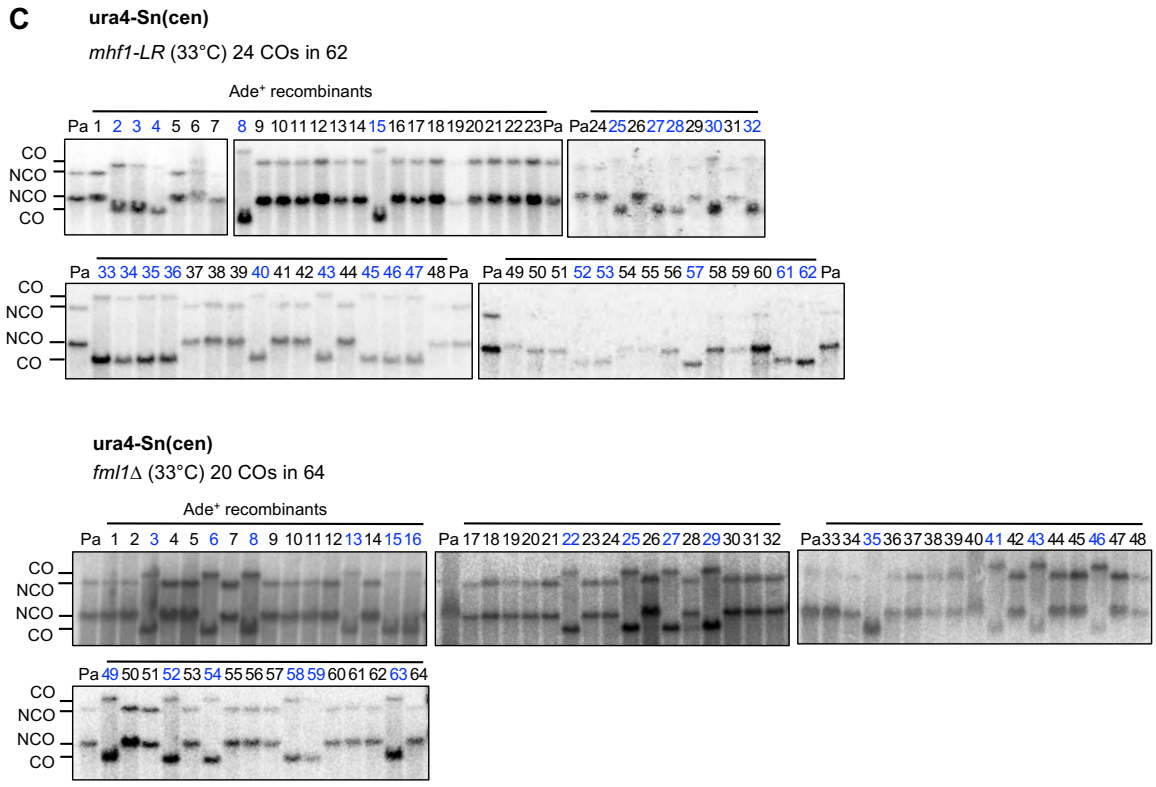

Supplementary Figure S12. Crossovers and non-crossovers in the *mhf1-L78R* and *fml1*Δ mutants. (A) Recombination rates in the cen1-Sn construct in wild type, *mhf1-LR,* and *fml1*Δ strains (TNF3347, 5444, and 5353, respectively) and in the ura4-Sn(cen) construct in wild type, *mhf1-LR,* and *fml1*Δ strains (TNF4684, 5455, and 4806, respectively). (B) Physical detection of crossovers and non-crossovers in the cen1-Sn construct in the *mhf1-LR* and *fml1*Δ mutants. (C) Physical detection of crossovers and non-crossovers in the ura4-Sn(cen) construct in the *mhf1-LR* and *fml1*Δ mutants.

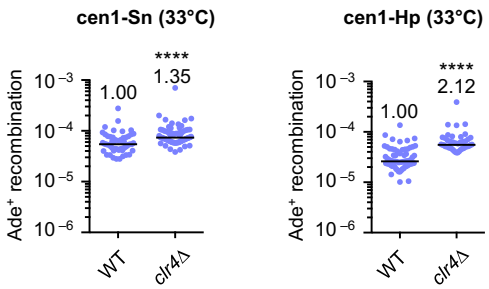

Supplementary Figure S13. A *clr4* deletion increases the recombination rate in centromeres. Recombination rates were determined in the cen1-Sn construct in wild type and *clr4*Δ strains (TNF3347 and 3734, respectively) as well as in the cen1-Hp construct in wild type and *clr4*Δ strains (TNF3144 and 3550, respectively).

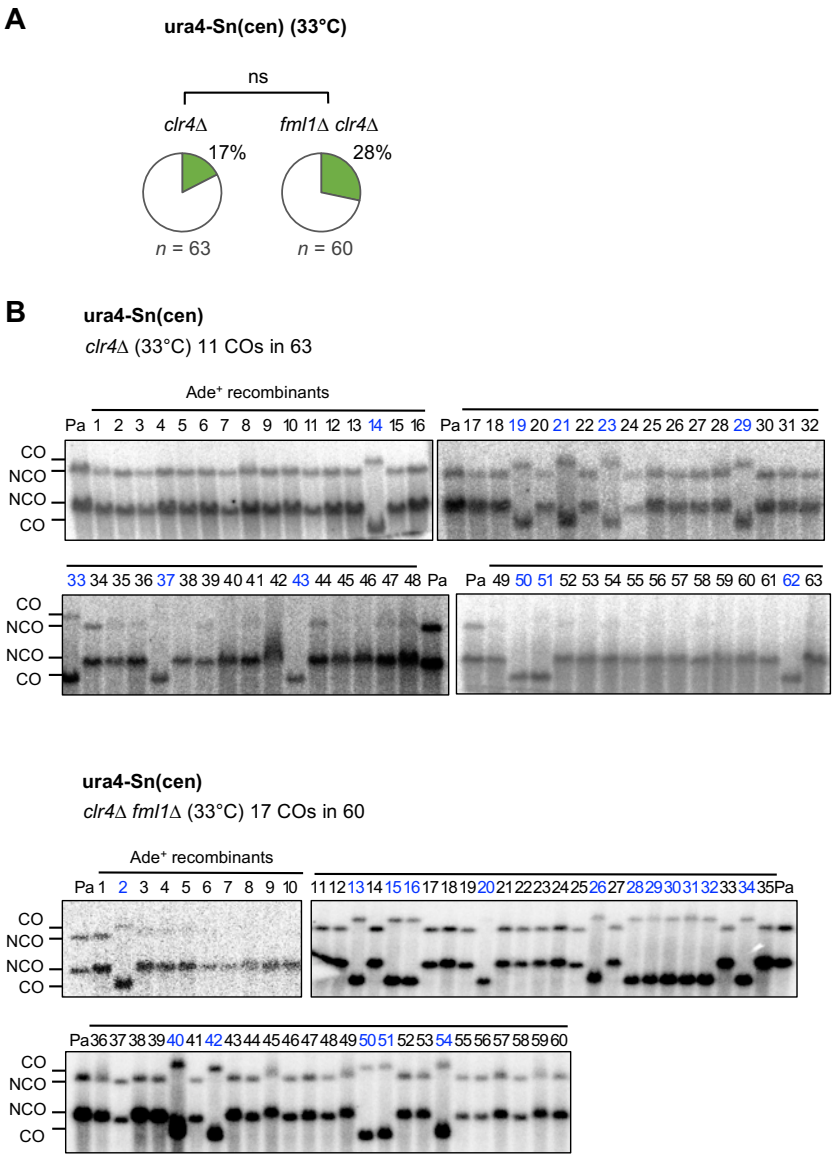

Supplementary Figure S14. Crossovers and non-crossovers in the ura4-Sn(cen) construct in the *clr4*Δ and *fml1*Δ*clr4*Δ mutants. (A) Proportions of crossovers in *clr4*Δ and *clr4*Δ*fml1*Δ mutants (TNF5281 and 5464, respectively) are indicated in pie charts. *P*-values were obtained by the two-tailed Fisher's exact test. *n*, sample number; ns, statistically non-significant. (B) Physical detection of crossovers and non-crossovers in the *clr4*Δ and *clr4*Δ *fml1*Δ mutants.

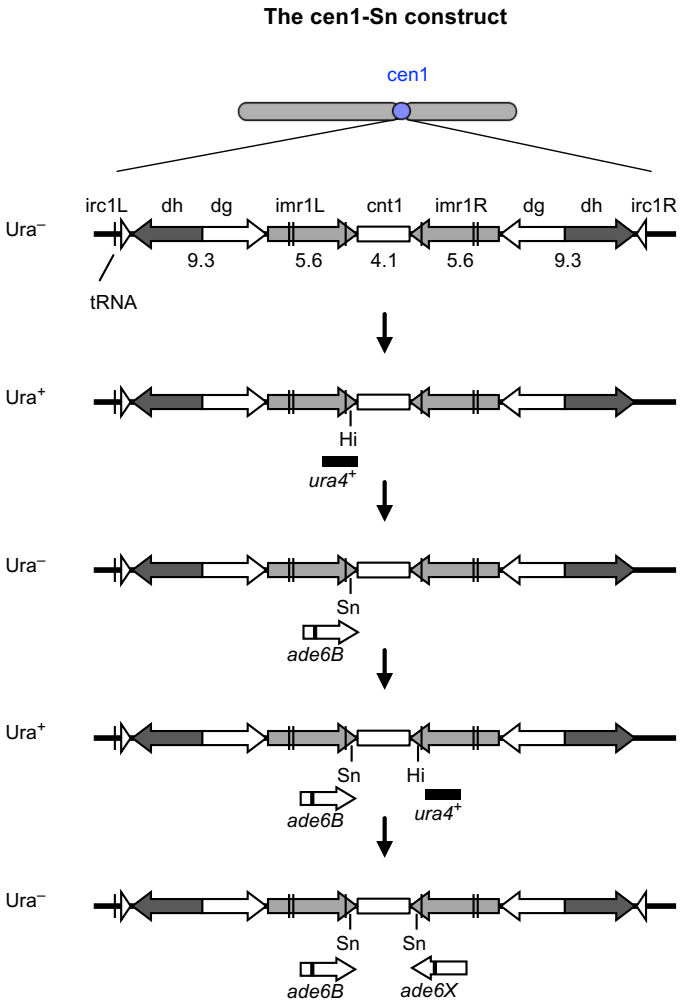

Supplementary Figure S15. Creation of the cen1-Sn construct. *ade6B* and *ade6X* heteroalleles were introduced at each side of imr repeats by a series of transformation. The *uar4*⁺ gene was introduced at the Hi site in imr1L. Then, the *ura4*⁺ gene was replaced by the DNA fragment containing the *ade6B* gene at the Sn site. Similarly, the *uar4*⁺ gene was introduced at the Hi site in imr1R. The *ura4*⁺ gene was then replaced by the DNA fragment containing the *ade6X* gene at the Sn site. Hi, HindIII; Sn, SnaBI.

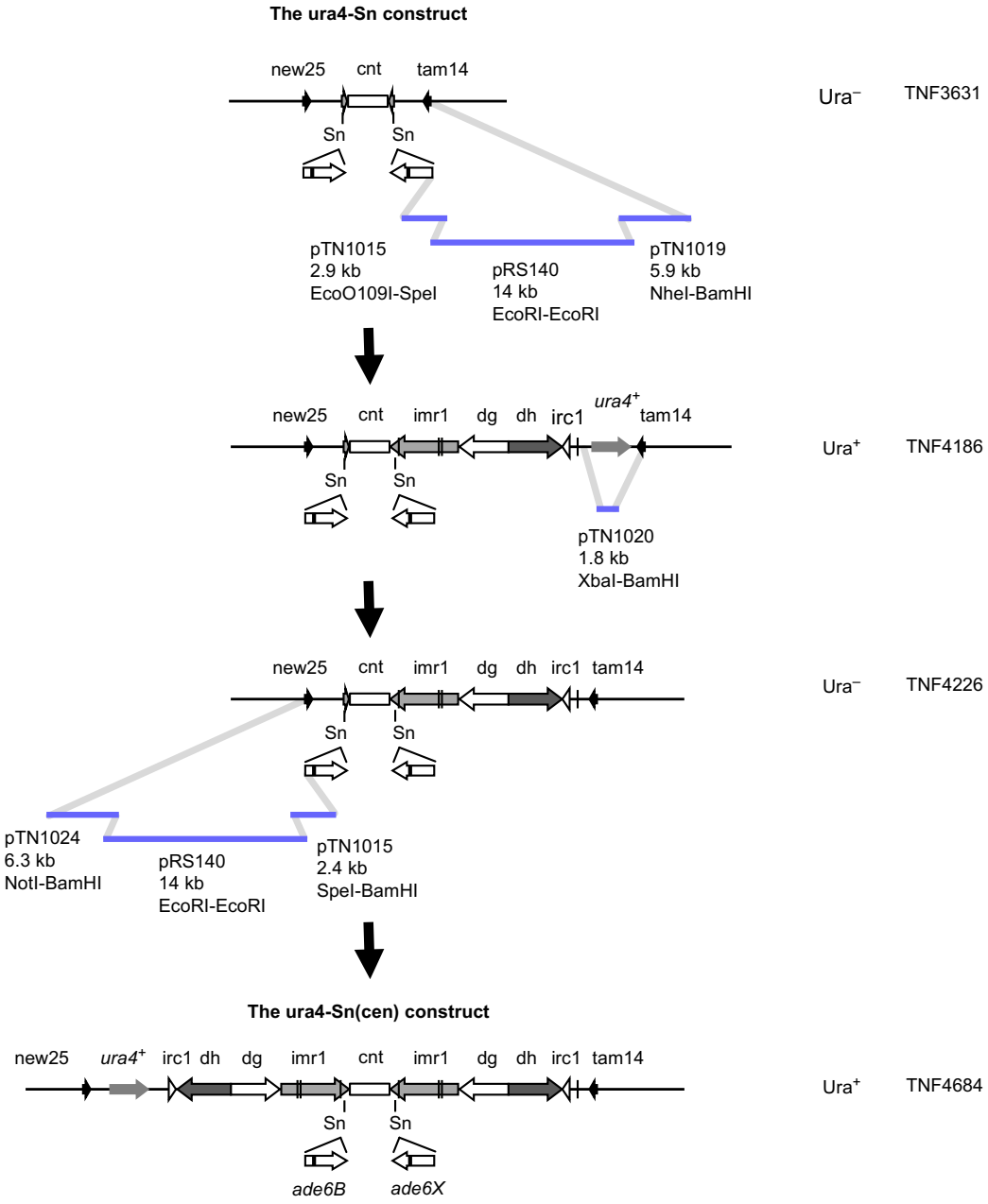

Supplementary Figure S16. Generation of the ura4-Sn(cen) construct. To introduce the entire cen1 sequence into the ura4 locus, a series of transformations of the ura4-Sn strain (TNF3631) was carried out. The DNA fragments used in the yeast transformation are indicated as blue bars. The right side of cen1 and the *ura4*$^{+}$ gene were introduced at the ura4 locus. After removal of the *ura4*$^{+}$ gene, the left side of cen1 and the *ura4*$^{+}$ gene were introduced at the ura4 locus.

Supplementary Table S1. Fission yeast strains used in this study.

strain	genotype
TNF3347	*h+, ade6Δ-D, imr1L(Sn:ade6B), imr1R(Sn:ade6X)*
TNF3446	*h+, ade6Δ-D, imr1L(Sn:ade6B), imr1R(Sn:ade6X), rad51::kanMX6*
TNF3452	*h+, ade6Δ-D, imr1L(Sn:ade6B), imr1R(Sn:ade6X), rad54::kanMX6*
TNF3459	*h+, ade6Δ-D, imr1L(Sn:ade6B), imr1R(Sn:ade6X), rad52::kanMX6*
TNF3631	*h+, ade6Δ-D, ura4::ade6B-cen1(Sn-Sn)-ade6X*
TNF3635	*h+, ade6Δ-D, ura4::ade6B-cen1(Sn-Sn)-ade6X, rad51::kanMX6*
TNF3645	*h+, ade6Δ-D, ura4::ade6B-cen1(Sn-Sn)-ade6X, rad54::kanMX6*
TNF3643	*h+, ade6Δ-D, ura4::ade6B-cen1(Sn-Sn)-ade6X, rad52::kanMX6*
TNF3144	*h+, ade6Δ-D, imr1L(Hp:ade6B), imr1R(Hp:ade6X)*
TNF3257	*h+, ade6Δ-D, imr1L(Hp:ade6B), imr1R(Hp:ade6X), rad51::kanMX6*
TNF3286	*h+, ade6Δ-D, imr1L(Hp:ade6B), imr1R(Hp:ade6X), rad54::kanMX6*
TNF3277	*h+, ade6Δ-D, imr1L(Hp:ade6B), imr1R(Hp:ade6X), rad52::kanMX6*
TNF3650	*h+, ade6Δ-D, ura4::ade6B-cen1(Hp-Hp)-ade6X*
TNF3664	*h+, ade6Δ-D, ura4::ade6B-cen1(Hp-Hp)-ade6X, rad51::kanMX6*
TNF3670	*h+, ade6Δ-D, ura4::ade6B-cen1(Hp-Hp)-ade6X, rad54::kanMX6*
TNF3667	*h+, ade6Δ-D, ura4::ade6B-cen1(Hp-Hp)-ade6X, rad52::kanMX6*
TNF3734	*h+, ade6Δ-D, imr1L(Sn:ade6B), imr1R(Sn:ade6X), clr4::kanMX6*
TNF3550	*h+, ade6Δ-D, imr1L(Hp:ade6B), imr1R(Hp:ade6X), clr4::kanMX6*
TNF4684	*h+, ade6Δ-D, ura4+: cen1(imr1L(Sn:ade6B), imr1R(Sn:ade6X))*
TNF5814	*h+, ade6Δ-D, ura4+: cen1(imr1L(Sn:ade6B), imr1R(Sn:ade6X)), rad51::kanMX6*
TNF5826	*h+, ade6Δ-D, ura4+: cen1(imr1L(Sn:ade6B), imr1R(Sn:ade6X)), rad54::kanMX6*
TNF5829	*h+, ade6Δ-D, ura4+: cen1(imr1L(Sn:ade6B), imr1R(Sn:ade6X)), rad52::kanMX6*
TNF3736	*h+, ade6Δ-D, imr1L(Sn:ade6B), imr1R(Sn:ade6X), cnp1-76*
TNF4656	*h+, ade6Δ-D, imr1L(Sn:ade6B), imr1R(Sn:ade6X), mis16-53*
TNF5534	*h+, ade6Δ-D, imr1L(Sn:ade6B), imr1R(Sn:ade6X), cnp20-M447T::kanMX6*
TNF4657	*h+, ade6Δ-D, imr1L(Sn:ade6B), imr1R(Sn:ade6X), mis18-262*
TNF5376	*h+, ade6Δ-D, imr1L(Sn:ade6B), imr1R(Sn:ade6X), mis14-271*
TNF4139	*h+, ade6Δ-D, imr1L(Sn:ade6B), imr1R(Sn:ade6X), csm1::kanMX6*
TNF4115	*h+, ade6Δ-D, imr1L(Sn:ade6B), imr1R(Sn:ade6X), cnp3::kanMX6*
TNF4779	*h+, ade6Δ-D, imr1L(Sn:ade6B), imr1R(Sn:ade6X), mhf1::hphMX6*
TNF5082	*h+, ade6Δ-D, imr1L(Sn:ade6B), imr1R(Sn:ade6X), mhf2::hphMX6*
TNF5353	*h+, ade6Δ-D, imr1L(Sn:ade6B), imr1R(Sn:ade6X), fml1::hphMX6*
TNF5128	*h+, ade6Δ-D, imr1L(Sn:ade6B), imr1R(Sn:ade6X), mhf1::hphMX6, fml1::kanMX6*
TNF5444	*h-, ade6Δ-D, imr1L(Sn:ade6B), imr1R(Sn:ade6X), mhf1-L78R*
TNF5455	*h+, ade6Δ-D, ura4+: cen1(imr1L(Sn:ade6B), imr1R(Sn:ade6X)), mhf1-L78R*
TNF4806	*h+, ade6Δ-D, ura4+: cen1(imr1L(Sn:ade6B), imr1R(Sn:ade6X)), fml1::hphMX6*
TNF3896	*h-, smt0, ade6Δ-D, ura4-D18, leu1-32, ChL (ubcp4::LEU2+::chk1, spcc1322::ura4, ade6+)*
TNF5477	*h-, smt0, ade6Δ-D, ura4-D18, leu1-32, ChL (ubcp4::LEU2+::chk1, spcc1322::ura4, ade6+), mhf1-L78R*
TNF4813	*h-, smt0, ade6Δ-D, ura4-D18, leu1-32, ChL (ubcp4::LEU2+::chk1, spcc1322::ura4, ade6+), fml1::hphMX6*
TNF5281	*h+, ade6Δ-D, ura4+: cen1(imr1L(Sn:ade6B), imr1R(Sn:ade6X)), clr4::hphMX6*
TNF5464	*h+, ade6Δ-D, ura4+: cen1(imr1L(Sn:ade6B), imr1R(Sn:ade6X)), fml1::hphMX6, clr4::kanMX6*
TNF35	*h+*
TNF5485	*h+, cnp20-M447T::kanMX6*
TNF3562	*h+, ade6Δ-D, ade6B::ura4+::ade6X*
TNF4186	*h-, ade6Δ-D, ura4+: cen1(Sn:ade6B, imr1R(Sn:ade6X)), swi6::kanMX6*
TNF4226	*h-, ade6Δ-D, ura4: cen1(Sn:ade6B, imr1R(Sn:ade6X)), swi6::kanMX6*

Supplementary Table S2. PCR primers used in this study.

Primer	Sequence	Real-time PCR target
ade6-D-D-F	5’ -GCTCGTACCGCAGCTTCAAG	ade6
ade6-D-D-R	5’ -GCAACCATACCAGGCAAATGA	ade6
imr1-in-F	5’ -ATTTCCGCTTACAAAATGCCA	imr-in
imr1-in-R	5’ -TTTCTCAACAGCAAAGCCTGAA	imr-in
imr1-out-F	5’ -GATGATATCGAGGCTTTCGGTTT	imr-out
imr1-out-R	5’ -TGTCCCTTCTGTTAAATTCTCGTGTA	imr-out
cnt1/3-F	5’ -CAACCACTGAAAGCGAATCTGTA	cnt1
cnt1/3-R	5’ -ATTCTGTAAGTTTGCTGTGCTTTATATCA	cnt1
adl1-F	5’ -AAATATGGCGATCCAGGAGATG	adl1
adl1-R	5’ -GCTTAACGTGCGCACAGACA	adl1
cnt2-F	5’ -TGCCTCTCCCTTGCCAGTAA	cnt2
cnt2-R	5’ -TCGTTGCGGTGTTTTGAAAA	cnt2
dg-F	5’ -TTGCACTCGGTTTCAGCTAT	dg
dg-R	5’ -TGCTCTGACTTGGCTTGTCT	dg
imr3-in2	5' -AAGTTTTGATGCTCAACAAATGGC	n.a.
cnt3R	5' -CGGAATTAGAAAGATTGATGATTTG	n.a.
cnt3L	5' -AACCGCAACAAACGATTAGC	n.a.
irc3F-long	5' -CATTAAAAATCAACAAGTCTTGTCCGTC	n.a.
irc3R-long	5' -ATAGAAACATTTTTGAGTGTTGTTCAGG	n.a.
cm-ade6	5' -TTGCTCCTCGGCCTCACAATTCAGG	n.a.
NotI-NheI-otr1R	5' -GGCGGCCGCTTCCAGCTTTTACATGCTAGCC	n.a.
irc1R-BlpI	5' -GGGCTAAGCCAGATTAGATTTCGGTGCGGTGC	n.a.
per1-Spe	5' -CCGTCTTCGTAACTAGTTCGCACTCACTG	n.a.
otr-Bam	5' -GCAATTGGATCCGTAAATAGGCGAGATC	n.a.

n.a., not applicable.